

Supporting Information

Photocontrol of Charge Injection/Extraction at Electrode/Semiconductor Interfaces for High-Photoresponsivity Organic Transistors

Hongtao Zhang,^{‡^a¶} Hongliang Chen,^{‡^a} Wei Ma,^b Jingshu Hui,^a Sheng Meng,^b Wei Xu,^c

Daoben Zhu^c and Xuefeng Guo^{*a}

^aBeijing National Laboratory for Molecular Sciences, State Key Laboratory for Structural Chemistry of Unstable and Stable Species, College of Chemistry and Molecular Engineering, Peking University, Beijing 100871, P. R. China. E-mail: guoxf@pku.edu.cn

^bInstitute of Physics, Chinese Academy of Sciences, Beijing 100190, P.R. China.

^cKey Laboratory of Organic Solids, Beijing National Laboratory for Molecular Science, Institute of Chemistry, Chinese Academy of Sciences, Beijing 100190, P. R. China.

[¶]Current position: School of Materials Science and Engineering, State Key Laboratory and Institute of Elemento-Organic Chemistry, Collaborative Innovation Center of Chemical Science and Engineering (Tianjin), Nankai University, Tianjin 300071, P. R. China.

[‡]These authors contributed equally.

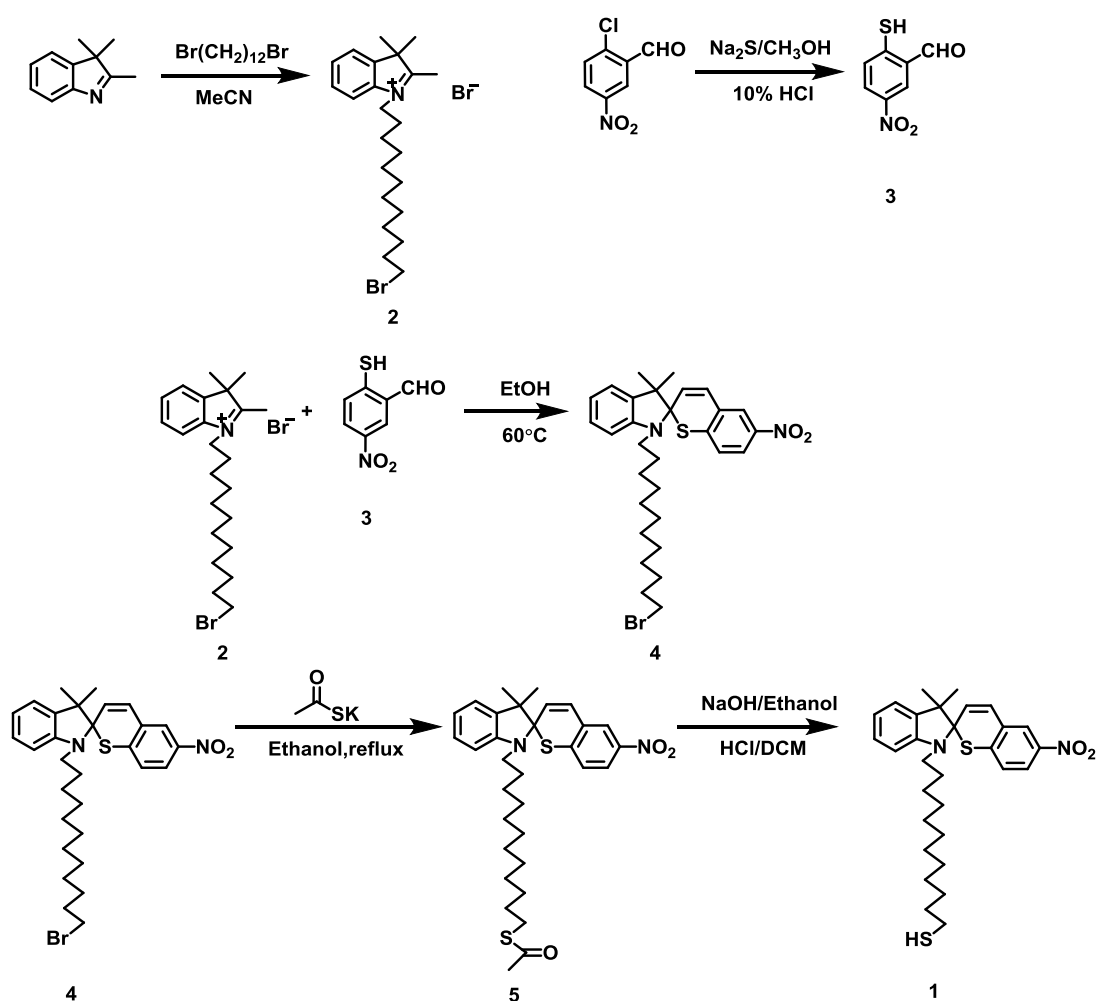
This file includes:

- Synthesis of alkanethiol-terminated spirothiopyran (SP-SH)
- Calculation Method for the Percent Conversion of SPs
- Calculation Method for the dipole moment of SP-closed and SP-open isomers
- Scheme S1
- Figs. S1 to S8

Experimental Section

Synthesis of alkanethiol-terminated spirothiopyran (SP-SH)

An alkanethiol-terminated spirothiopyran was straightforwardly synthesized as shown in Scheme S1. Chemical reagents used for synthesis were purchased from Aldrich Chemical Co. unless otherwise indicated. All solvents were purified by standard methods. ^1H NMR spectra of the samples were recorded on a Mercury Mercury Plus spectrometer (300 MHz).



Scheme S1. Synthetic route for an alkanethiol-terminated spirothiopyran **1**.

Synthesis of N-(12-bromododecyl)-2,3,3-trimethylindolenium bromide (2). 1,12-dibromododecane (3.28 g, 10 mmol) and 2,3,3-trimethylindolenin (1.58 ml, 10 mmol) were

dissolved in 5 mL of acetonitrile and refluxed for 72 h. After cooling down to room temperature, the solution was evaporated under reduced pressure. The solid formed was precipitated with ether three times to give a red-purple solid of **2** (4.14 g, 8.49 mmol) in 84.9% yield. This compound was used in the next step without any further purification. ¹H NMR (300 MHz, CDCl₃, δ): 7.62–7.54 (m, 4H, CH), 4.68 (t, 2H, CH₂), 3.35 (t, 2H, CH₂), 3.10 (s, 3H, CH₃), 2.18 (t, 2H, CH₂), 1.86 (m, 2H, CH₂), 1.79 (m, 2H, CH₂), 1.66 (s, 6H, CH₃), 1.46–1.23 (m, 22H, CH₂). MS (ESI, m/z): 485.4 M-Br⁺.

Synthesis of 2-mercapto-5-nitrobenzaldehyde (3). 2-chloro-5-nitrobenzaldehyde (1.85 g, 10 mmol) was dissolved in 15 mL methanol, and the solution was heated to 50 °C. Na₂S • 9H₂O (2.4g, 10 mmol) in 10 mL methanol was dropped into the above solution, then the reaction solution was cooled down to 0~5 °C. After that, the reaction solution was adjusted to acidic (pH = 1). The obtained precipitate was filtered and then dried in vacuum to give yellow solid of **3** (1.3 g, 7.10 mmol) in 70.1%. ¹H NMR (300 MHz, CDCl₃, δ): 10.10 (s, 1H, CHO), 8.61 (d, 1H, CH), 8.22 (m, 1H, CH), 7.48 (d, 1H, CH), 6.15 (s, 1H, SH). MS (ESI, m/z): 182.2 M-H⁺.

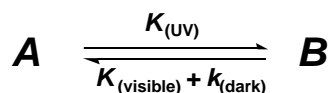
Synthesis of 1-(12-bromododecyl)-3,3-dimethyl-6'-nitrospiro[indoline-2,2'-thiochromene (4). Compound **2** (4.05g, 10 mmol) and Compound **3** (2.20 mg, 12 mmol) were dissolved in 30 mL of ethanol. After 5 h reflux, the reaction solution was cooled down to room temperature. The precipitate was filtered. The solid was dissolved in CH₂Cl₂ and purified by column chromatography with an eluent of hexane: ethyl acetate = 8:1. The obtained solid was recrystallized from ethanol three times to give yellow crystals of **4** (4.71 g, 8.25 mmol) in 82.5%. ¹H NMR (300 MHz, CDCl₃, δ): 8.02 (d, 1H, CH), 7.91 (dd, 1H, CH), 7.23 (d, 1H, CH), 7.15 (m, 1H, CH), 7.06 (d, 1H, CH), 6.85 (m, 2H, CH), 6.52 (d, 1H, CH), 5.99 (d, 1H, CH), 3.40 (t,

2H, CH₂), 3.25–2.97 (m, 2H, CH₂), 1.88–1.81 (m, 2H, CH₂), 1.65–1.56 (m, 2H, CH₂), 1.38 (s, 3H, CH₃), 1.36–1.25 (m, 16H, CH₂), 1.23 (s, 3H, CH₃); MS (ESI, m/z): 572.2 M-H⁺.

Synthesis of 1-(12-thioldodecyl)-3,3-dimethyl-6'-nitrospiro[indoline-2,2'-thiochromene (I). Thioacetic acid potassium salt (3.43g, 30 mmol) and Compound 4 (4.71 g, 8.25 mmol) were stirred in ethanol solution for 0.5 h under reflux. The resulting dark red solution was filtered, and KOH in ethanol was added (the molar ratio of KOH to 2 was 2:1). The solution was then stirred at room temperature under argon for 2h, filtered, and evaporated to dryness. The yellow crude product was dissolved in CH₂Cl₂. The resulting solution was washed with an aqueous HCl solution (pH = 4.0) and evaporated to dryness. The crude product was purified by column chromatography with an eluent of hexane: ethyl acetate = 16:1. The obtained solid was recrystallized from ethanol three times to give yellow crystals of **1** (3.10 g, 5.92 mmol) in 71.8%. ¹H NMR (400 MHz, CDCl₃, δ): 8.01 (d, J = 2.4Hz, 1H), 7.91 (dd, J = 8.7, 1H), 7.23 (d, J = 7.0, 1H), 7.14 (m, 1H), 7.06 (d, J = 7.2, 1H), 6.84 (m, 2H), 6.51 (d, J = 7.7, 1H), 5.99 (d, J = 10.9, 1H), 3.25–2.96 (m, 2H), 2.67 (t, J = 7.2, 2H), 1.78–1.62 (m, 7H), 1.45 (s, 3H), 1.38–1.25 (m, 14H), 1.22 (s, 3H); MS (ESI) m/z (%) 523.24 M-H⁺.

Calculation Method for the Percent Conversion of SPs

Photochromism is defined as a reversible change in a chemical species between two forms.



To calculate the percent conversion (x_c) of SP molecules from SP-close (**A**) to SP-open (**B**), a semiempirical approach is used, assuming that a pseudo-first-order process with linear intensity dependence adequately describes the present photochromic system.¹ In solid, the thermal

conversion from SP-close (**A**) to SP-open (**B**) may be neglected. SP-open (**B**) may be a mixture of several stereoisomers of the merocyanine form and their aggregates. Then the overall change in concentration of SP-open (**B**) with time can be simply given by the following rate equation: $-dB/dt = K_{(visible)}B - K_{(UV)}A + K_{(dark)}B = K_{(visible)}A_0x - K_{(UV)}A_0(1-x) + K_{(dark)}A_0x$ where A and B are the concentrations of SP-close and SP-open, $K_{(UV)}$ and $K_{(visible)}$ are the photochemical rate constants, $K_{(dark)}$ is the thermal rate constant for conversion from SP-open to SP-close, and A_0 is the total concentration of all the SP molecules. At the photostationary state, the percent conversion (x_e) of SP molecules from SP-close to SP-open can be calculated through the following relationship:

$$\frac{x_e}{1-x_e} = \frac{K_{(UV)}}{K_{(visible)} + K_{(dark)}}$$

In the case of SP in the DMF solution, the rate constants for each process are $K_{(UV-spectrum)} = \sim 4.4 \pm 0.5 \times 10^{-3} \text{ s}^{-1}$, $K_{(visible-spectrum)} = \sim 2.9 \pm 0.1 \times 10^{-3} \text{ s}^{-1}$ and $K_{(dark-spectrum)} = \sim 0.31 \pm 0.1 \times 10^{-3} \text{ s}^{-1}$ (data in the dark unshown) (Figure S1). As a result, the calculated percent conversion (x_e) of SP molecules from SP-close to SP-open at the photostationary state is $\sim 57.9\%$.

Calculation Method for the dipole moment of SP-closed and SP-open isomers

All computations were performed using Gaussian 09.² The geometry of both SP-closed and SP-open forms were optimized with a basic STO-3G ab initio basis set, then the dipole moment of each isomer was calculated at the B3LYP/6-31 Gd basis set. $\mu_{\perp,SAM} = Dipole_x \times \cos \alpha$. SP-SH adopt an approximate off-normal tilt, α of 35° .

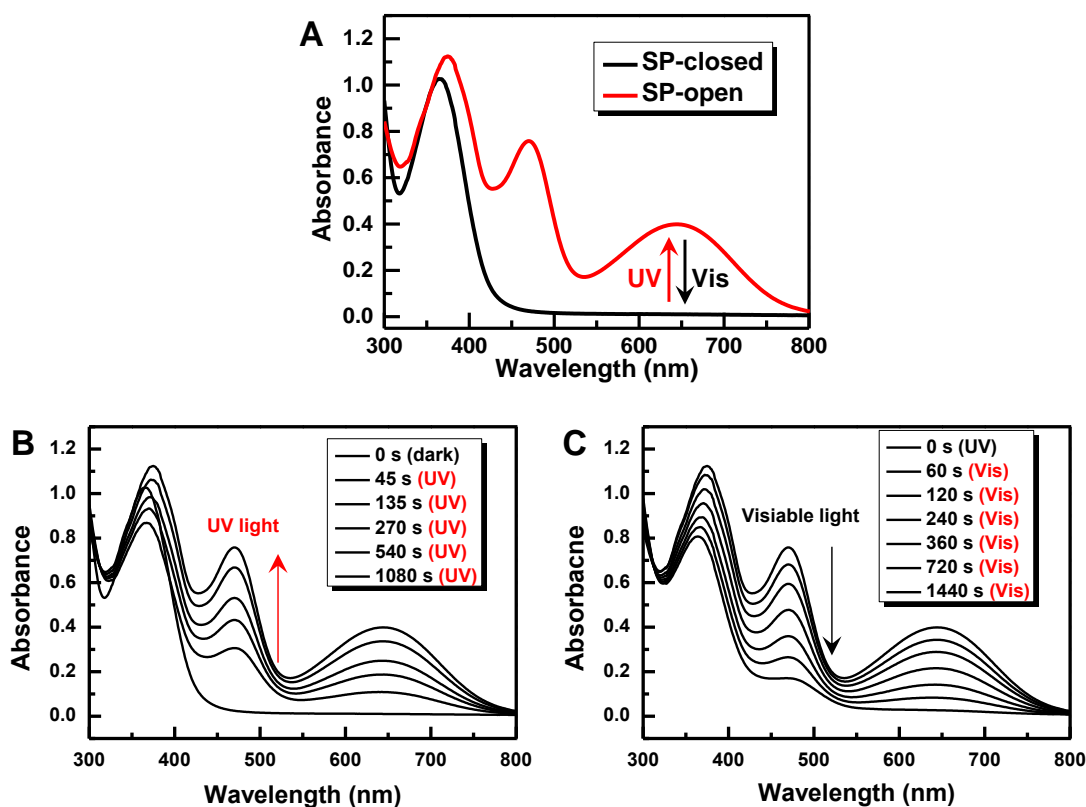


Fig. S1 (A) UV–Vis absorption spectra of SP-SH in DMF solution (10^{-4} M) under irradiation with lights of different wavelengths (UV: red, and vis: black). Gradual transitions of UV-Visible absorption spectra of SP-SHs in DMF solution under UV (B) and visible light (C) irradiation.

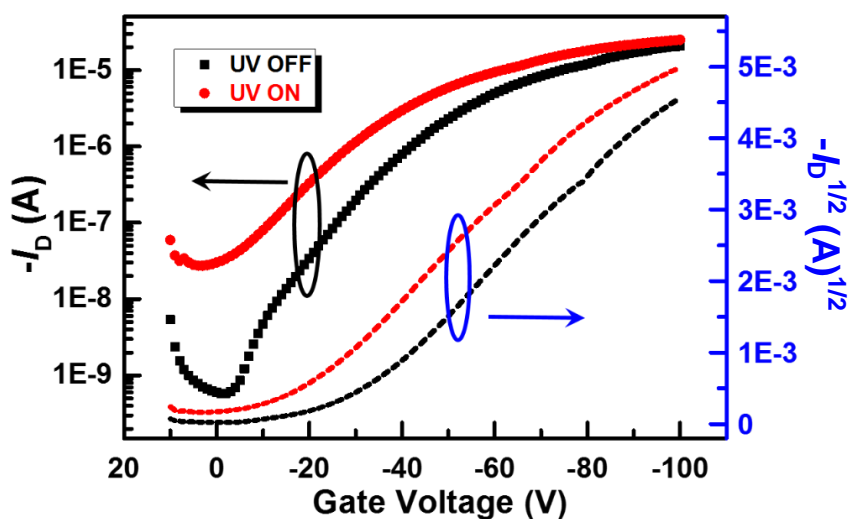


Fig. S2 Representative transfer characteristics of pentacene devices on silicon wafer substrates with SP-SH SAMs on Au electrodes before and after UV irradiation.

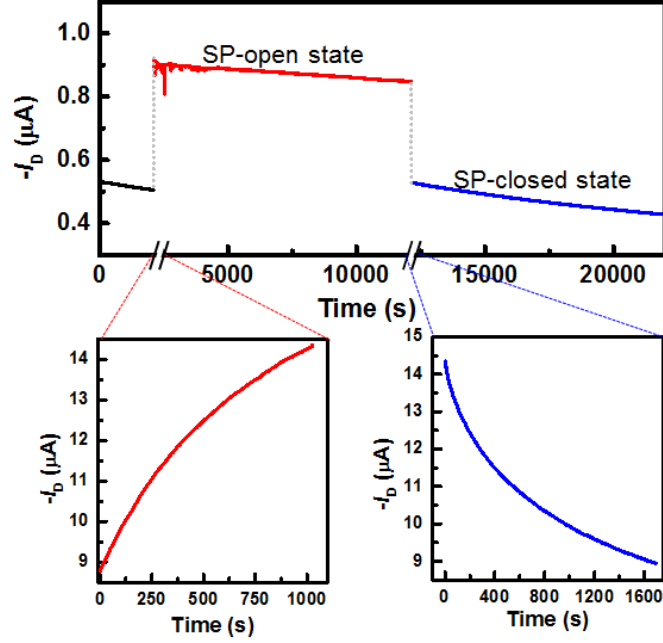


Fig. S3 Real-time measurements of I_D to test the dark stability of both SP-open and SP-closed states. Insets show the UV (left, red) and Vis (right, blue) light programming processes, respectively. UV light: $\lambda = 365$ nm, $\sim 10 \mu\text{W cm}^{-2}$; Vis light: $\lambda > 520$ nm, $\sim 30 \text{ mW cm}^{-2}$.

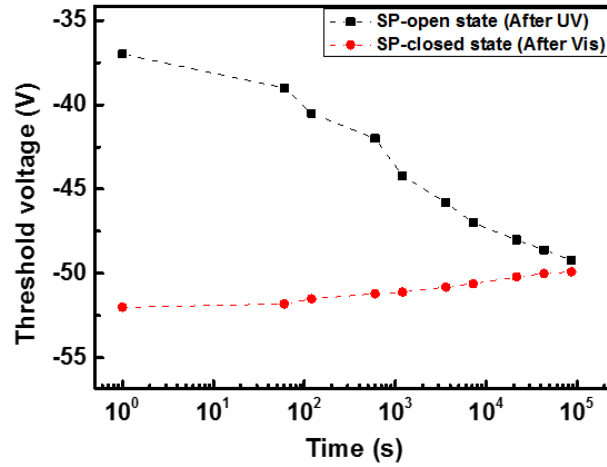


Fig. S4 Retention characteristics of the memory device. Threshold voltage (V_{th}) is the second method to read information and evaluate the retention ability of a memory device. At $V_D = -100$ V, V_G scanned from +20 V to -100 V. After over 24 h, the V_T window (ΔV_T) vanishes (smaller than 1 V). The SP-open state was preset by UV light illumination ($\lambda = 365$ nm, $\sim 10 \mu\text{W cm}^{-2}$, approximately 600 s), while the SP-closed state was preset by white light illumination ($\lambda > 520$ nm, $\sim 30 \text{ mW cm}^{-2}$, approximately 900 s).

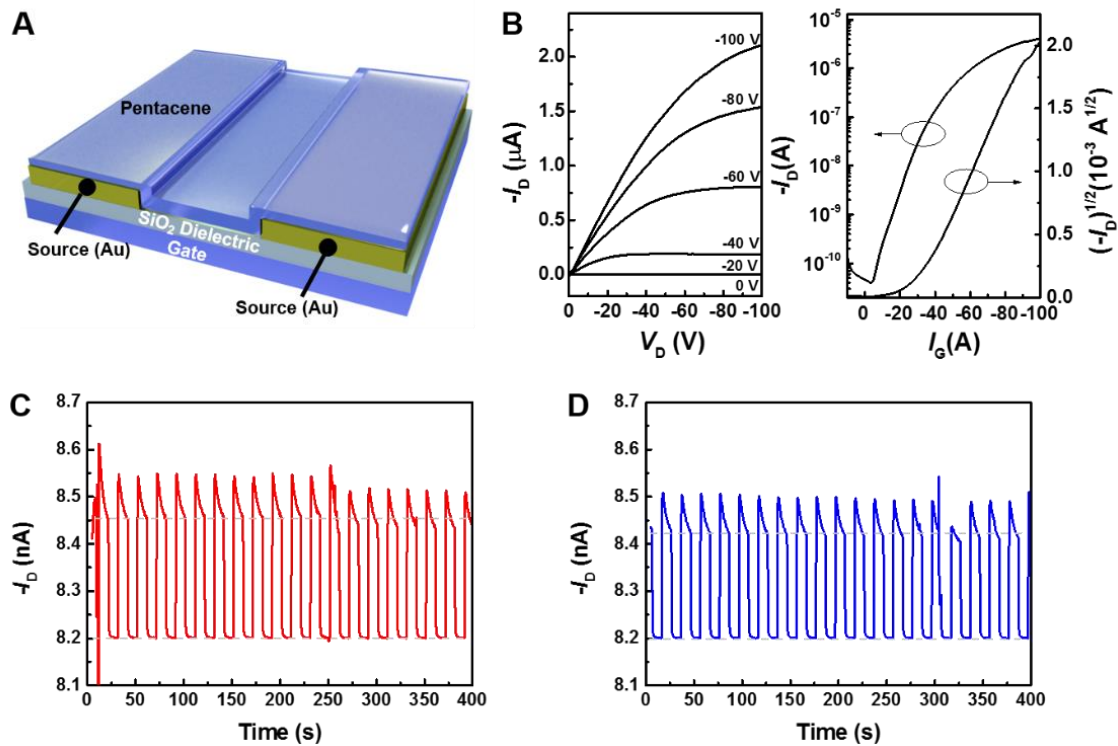


Fig. S5 Device photoresponses of a control device based on pristine pentacene without SP-SAMs under different conditions: (A) Device structure of the pentacene control device without SP-SAMs. (B) Representative output and transfer characteristics for a control device. An average mobility of $0.033 \pm 0.002 \text{ cm}^2 \text{ V}^{-1} \text{ s}^{-1}$ and an average on/off ratio of approximately 10^5 were achieved based on over 20 individual devices ($L = 120$ and $W = 2000 \text{ } \mu\text{m}$). (C) Device photoresponse to 365-nm UV light illumination ($\sim 10 \text{ } \mu\text{W cm}^{-2}$) and (D) white light illumination ($\lambda > 520 \text{ nm}$, $\sim 30 \text{ mW cm}^{-2}$). $V_D = -30 \text{ V}$ and $V_G = -15 \text{ V}$.

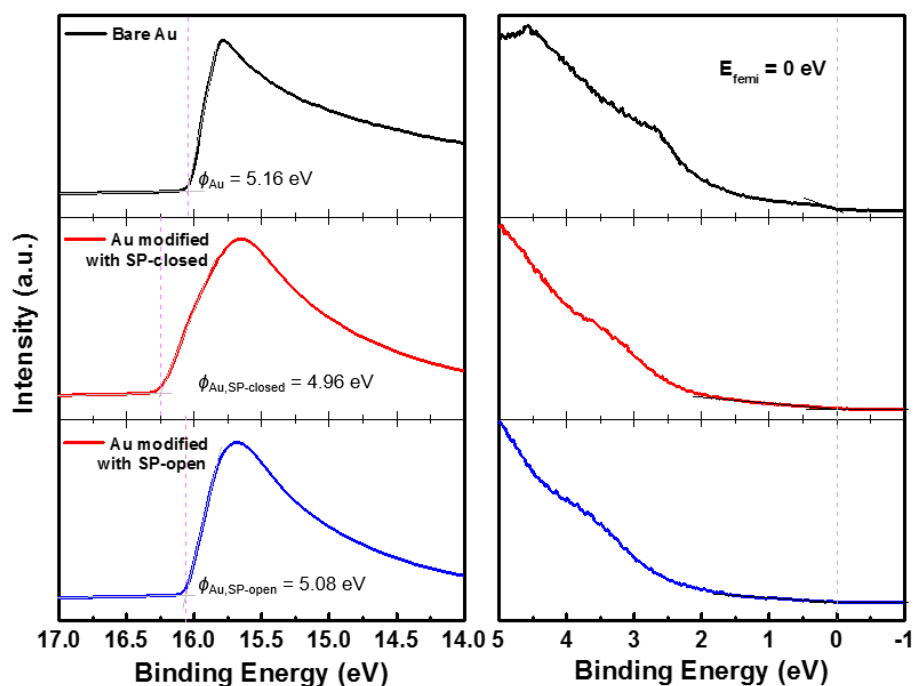


Fig. S6 UPS measurements for bare Au (black), and surfaces after modification with SP-closed (red) and SP-open (blue) SAMs. The left side of these spectra is a view of the secondary electron edge (SEE), while the right-hand part of these spectra is a view of valance band maximum (VBM) region. Shifts in the SEE energy are directly proportional to the surface work function change.

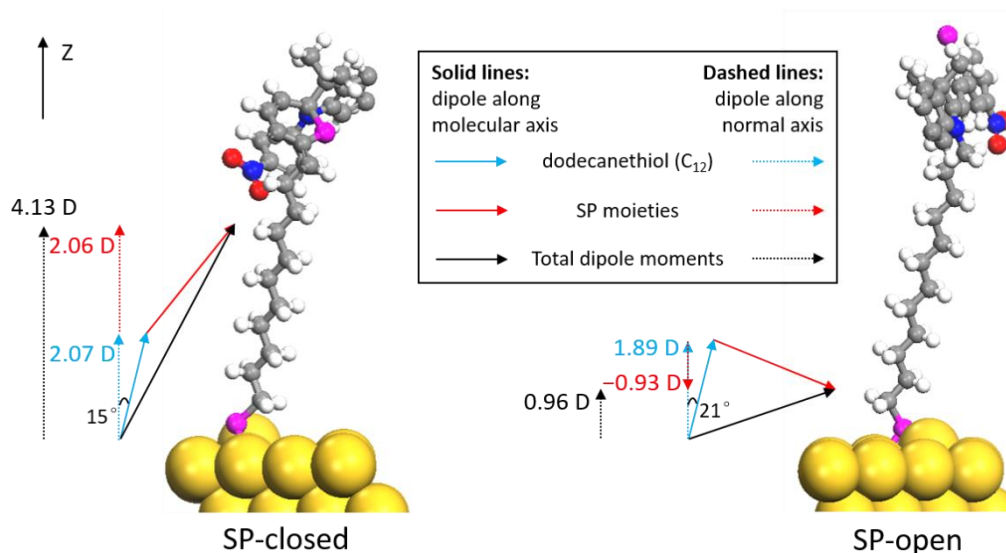


Fig. S7 Optimized geometry and calculated dipole moments of SP-closed and SP-open forms.

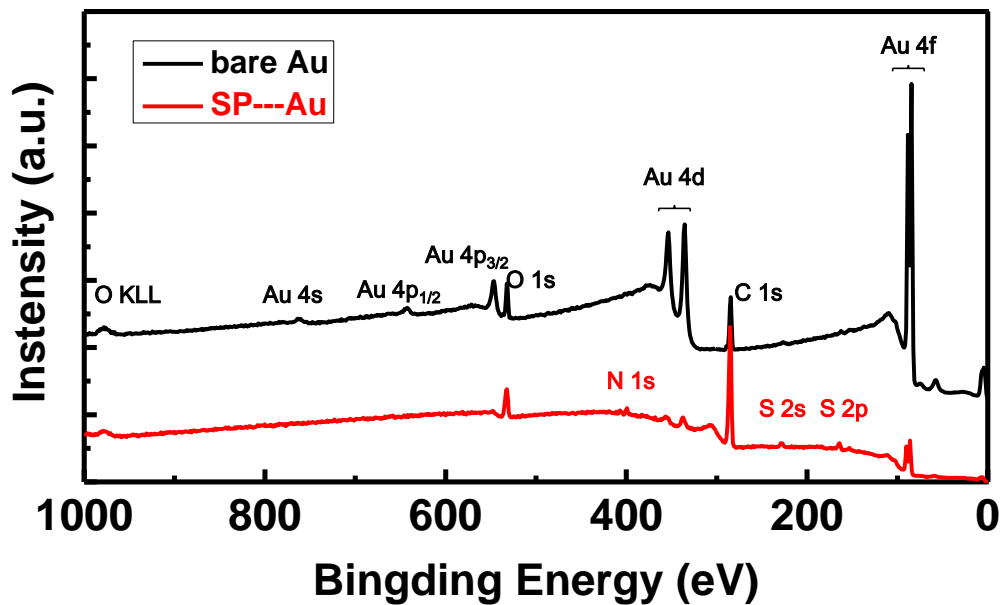


Fig. S8 XPS spectra for SP-SAM modified gold film and bare gold film. For the data of bare gold sample, the peaks at 84 and 88 eV are attributed to Au 4f, those at 335 and 353 eV are attributed to Au 4d, that at 546 eV is attributed to Au 4p, and that at 763 eV is attributed to Au 4s. For the SP-SAM modified sample, the peaks at 162 eV, 163 and 229 eV are attributed to S 2p and 2s, respectively.

References:

(1) G. Berkovic, V. Krongauz and V. Weiss, *Chem. Rev.* 2000, **100**, 1741–1754.

(2) Gaussian 09, Revision A.02

M. J. Frisch, G. W. Trucks, H. B. Schlegel, G. E. Scuseria, M. A. Robb, J. R. Cheeseman, G. Scalmani, V. Barone, B. Mennucci, G. A. Petersson, H. Nakatsuji, M. Caricato, X. Li, H. P. Hratchian, A. F. Izmaylov, J. Bloino, G. Zheng, J. L. Sonnenberg, M. Hada, M. Ehara, K. Toyota, R. Fukuda, J. Hasegawa, M. Ishida, T. Nakajima, Y. Honda, O. Kitao, H. Nakai, T. Vreven, J. A. Montgomery, Jr. J. E. Peralta, F. Ogliaro, M. Bearpark, J. J. Heyd, E. Brothers, K. N. Kudin, V. N. Staroverov, R. Kobayashi, J. Normand, K. Raghavachari, A. Rendell, J. C. Burant, S. S. Iyengar, J. Tomasi, M. Cossi, N. Rega, J. M. Millam, M. Klene, J. E. Knox, J. B. Cross, V. Bakken, C. Adamo, J. Jaramillo, R. Gomperts, R. E. Stratmann, O. Yazyev, A. J. Austin, R. Cammi, C. Pomelli, J. W. Ochterski, R. L. Martin, K. Morokuma, V. G. Zakrzewski, G. A. Voth, P. Salvador, J. J. Dannenberg, S. Dapprich, A. D. Daniels, O. Farkas, J. B. Foresman, J. V. Ortiz, J. Cioslowski and D. J. Fox, Gaussian, Inc., Wallingford CT, 2009.